



University of Groningen

## Origin of the reduced fill factor and photocurrent in MDMO-PPV

Mandoc, M. Magdalena; Veurman, Welmoed; Koster, L. Jan Anton; de Boer, Bert; Blom, Paul W. M.

*Published in:*  
Advanced Functional Materials

*DOI:*  
[10.1002/adfm.200601110](https://doi.org/10.1002/adfm.200601110)

**IMPORTANT NOTE:** You are advised to consult the publisher's version (publisher's PDF) if you wish to cite from it. Please check the document version below.

*Document Version*  
Publisher's PDF, also known as Version of record

*Publication date:*  
2007

[Link to publication in University of Groningen/UMCG research database](#)

### *Citation for published version (APA):*

Mandoc, M. M., Veurman, W., Koster, L. J. A., de Boer, B., & Blom, P. W. M. (2007). Origin of the reduced fill factor and photocurrent in MDMO-PPV: PCNEPV all-polymer solar cells. *Advanced Functional Materials*, 17(13), 2167-2173. <https://doi.org/10.1002/adfm.200601110>

### **Copyright**

Other than for strictly personal use, it is not permitted to download or to forward/distribute the text or part of it without the consent of the author(s) and/or copyright holder(s), unless the work is under an open content license (like Creative Commons).

### **Take-down policy**

If you believe that this document breaches copyright please contact us providing details, and we will remove access to the work immediately and investigate your claim.

*Downloaded from the University of Groningen/UMCG research database (Pure): <http://www.rug.nl/research/portal>. For technical reasons the number of authors shown on this cover page is limited to 10 maximum.*

DOI: 10.1002/adfm.200601110

# Origin of the Reduced Fill Factor and Photocurrent in MDMO-PPV:PCNEPV All-Polymer Solar Cells\*\*

By M. Magdalena Mandoc, Welmoed Veurman, L. Jan Anton Koster, Bert de Boer, and Paul W. M. Blom\*

The photogeneration mechanism in blends of poly[2-methoxy-5-(3',7'-dimethyloctyloxy)-1,4-phenylene vinylene] (MDMO-PPV) and poly[oxa-1,4-phenylene-(1-cyano-1,2-vinylene)-(2-methoxy-5-(3',7'-dimethyloctyloxy)-1,4-phenylene)-1,2-(2-cyanovinylene)-1,4-phenylene] (PCNEPV) is investigated. The photocurrent in the MDMO-PPV:PCNEPV blends is strongly dependent on the applied voltage as a result of a low dissociation efficiency of the bound electron-hole pairs. The dissociation efficiency is limited by low carrier mobilities, low dielectric constant, and the strong intermixing of the polymers, leading to a low fill factor and a reduced photocurrent at operating conditions. Additionally, electrons trapped in the PCNEPV phase recombine with the mobile holes in the MDMO-PPV phase at the interface between the two polymers, thereby affecting the open-circuit voltage and increasing the recombination losses. At an intensity of one sun, Langevin recombination of mobile carriers dominates over trap-assisted recombination.

## 1. Introduction

The efficiency of polymer-based solar cells has been increased significantly in the last years. In blends of regioregular poly(3-hexylthiophene) (P3HT) and [6,6]-phenyl-C<sub>61</sub>-butyric acid methyl ester (PCBM) that form bulk heterojunctions (BHJs), efficiencies of more than 4 % have been reported.<sup>[1–3]</sup> A disadvantage of this type of cell is that one of the components, namely PCBM, only weakly absorbs the visible part of the solar spectrum. In this respect, all-polymer blends are promising materials for organic photovoltaics, with visible-light absorption in both components. Initially, the efficiencies of all-polymer cells made with blends of poly(dialkoxy-*p*-phenylene vinylene) (PPV) derivatives exhibited efficiencies lower than 1 %.<sup>[4,5]</sup> However, recently the efficiencies of devices using PPV derivatives as a donor have been strongly increased. For an acceptor based on a red-emitting polyfluorene<sup>[6]</sup> or a cyano-substituted copolymer,<sup>[7]</sup> efficiencies of 1.5 % and 1.7 % have been reported, respectively. Clearly, these efficiencies start to

approach the 2.5 % of PPV derivatives when blended with fullerenes.<sup>[8]</sup>

Blends of poly[2-methoxy-5-(3',7'-dimethyloctyloxy)-1,4-phenylene vinylene] (MDMO-PPV) and poly[oxa-1,4-phenylene-(1-cyano-1,2-vinylene)-(2-methoxy-5-(3',7'-dimethyloctyloxy)-1,4-phenylene)-1,2-(2-cyanovinylene)-1,4-phenylene] (PCNEPV) form an efficient charge-transfer donor-acceptor system, because of the difference between their electron affinities (ca. 0.5 eV) and ionization potentials (ca. 0.7 eV).<sup>[5]</sup> Morphology studies show a strong intermixing of the two polymer phases with the size of the polymer domains formed in the blend not far from the exciton diffusion length.<sup>[5]</sup> Solar cells made of this blend have a large open-circuit voltage ( $V_{oc}$ ) of about 1.3–1.5 eV, and an optimized device, including an additional acceptor top layer and thermal treatment, shows an efficiency of about 0.75 %.<sup>[5]</sup>

However, the reason for the relatively poor performance of these devices, especially the unannealed ones, as compared to their fullerene counterparts is not clear. One of the main reasons for the relatively low efficiencies is the fact that the fill factor (FF) is less than 25 %, that is, about twice as low as for MDMO-PPV:PCBM devices. In earlier work on fullerene devices, we demonstrated that under reverse bias the shape of the photocurrent versus voltage is strongly dependent on the generation efficiency of free carriers from bound electron-hole (e-h) pairs.<sup>[9]</sup> The electric field and temperature dependence of the photocurrent can be described with a model based on Onsager's theory of geminate charge recombination. Furthermore, strongly unbalanced transport leads to the formation of space charge in the solar cell.<sup>[10]</sup> The resulting square-root dependence of the photocurrent on voltage also strongly reduces the FF of space-charge limited devices. In a recent study, the charge-transport properties of MDMO-PPV:PCNEPV blends (1:1 wt %) were investigated. Hole transport in the MDMO-PPV phase is space-charge limited and the hole mobility is equal to the value

[\*] Prof. P. W. M. Blom, M. M. Mandoc, W. Veurman, L. J. A. Koster, Dr. B. de Boer  
Molecular Electronics  
Zernike Institute for Advanced Materials  
University of Groningen  
Nijenborgh 4, NL-9747AG Groningen (The Netherlands)  
E-mail: p.w.m.blom@rug.nl  
M. M. Mandoc, L. J. A. Koster  
Dutch Polymer Institute (DPI)  
P.O. Box 902, 5600 AX Eindhoven (The Netherlands).

[\*\*] This work forms part of the research program of the Dutch Polymer Institute (DPI), project # 324. The authors acknowledge Dr. Sjoerd C. Veenstra of ECN for useful discussions and Dr. Marc M. Koetse and Jorgen Sweelssen of TNO Science and Industry for the supply of PCNEPV.

of the pristine polymer, being  $5 \times 10^{-10} \text{ m}^2 \text{ V}^{-1} \text{ s}^{-1}$  at room temperature. Electron transport in the PCNEPV phase is, however, strongly trap-limited.<sup>[11]</sup> The presence of electron traps leads to a highly unbalanced charge transport in this type of blend. In this work we address the possible causes of the low FF and resulting poor efficiency, and show the limiting mechanisms that must be overcome for future efficient all-polymer solar cells.

## 2. Results and discussion

### 2.1. The Photocurrent of MDMO-PPV:PCNEPV Solar Cells

An all-polymer BHJ solar cell consists of a polymer blend sandwiched between two electrodes. As a bottom electrode poly(3,4-ethylenedioxythiophene):poly(4-styrene sulphonate) (PEDOT:PSS) is spin-coated on transparent indium tin oxide (ITO)-coated glass to create an Ohmic contact for holes. For electrons, LiF/Al forms an Ohmic contact with the lowest unoccupied molecular orbital (LUMO) of the electron acceptor (PCNEPV). An exciton generated in the donor and/or acceptor phase can diffuse towards the interface between the two polymers. Subsequently, electron transfer to the acceptor (hole transfer to the donor) occurs because of the difference in electron affinities and ionization potentials of the two polymers. In this way, a bound e-h pair is formed across the interface, with the hole in the donor polymer and the electron in the acceptor polymer. Because of the low dielectric constants  $\epsilon_r$  of the organic materials ( $\epsilon_r$  ranges typically from 2 to 4), these e-h pairs are strongly bound by Coulomb interaction, with binding energies typically of several tenths of an electronvolt. This bound pair still needs to dissociate with the help of the internal electric field in the device in order to produce free carriers, which are then transported to the appropriate electrodes. In Figure 1, the current-density-voltage ( $J$ - $V$ ) characteristics measured in the dark ( $J_D$ ) and under illumination ( $J_L$ ) with  $1000 \text{ W m}^{-2}$  white light are shown for a typical MDMO-PPV:PCNEPV (1:1 weight ratio) solar cell, with an active layer thickness of 50 nm. The current under illumination is almost linear, with an apparent inward bend, resulting in a low FF.

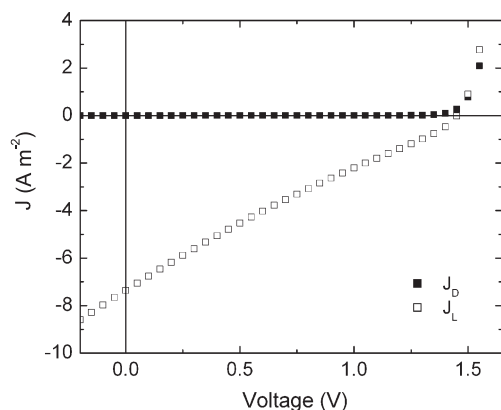


**Figure 1.** Typical dark (solid symbols) and illuminated (open symbols)  $J$ - $V$  characteristics of a MDMO-PPV:PCNEPV solar cell. The device was illuminated with  $1000 \text{ W m}^{-2}$  white light.

As a result, the high open-circuit voltage of MDMO-PPV:PCNEPV solar cells is counterbalanced by a low short-circuit current and low FF, leading to poor efficiencies. To study the dependence of the photocurrent on electric field we plotted in Figure 2 the photocurrent ( $J_{ph} = J_L - J_D$ ) of a typical MDMO-PPV:PCNEPV solar cell, against the effective applied voltage ( $V_0 - V$ ), where  $V_0$  is the compensation voltage, which is defined as the voltage for which the photocurrent  $J_{ph}$  is

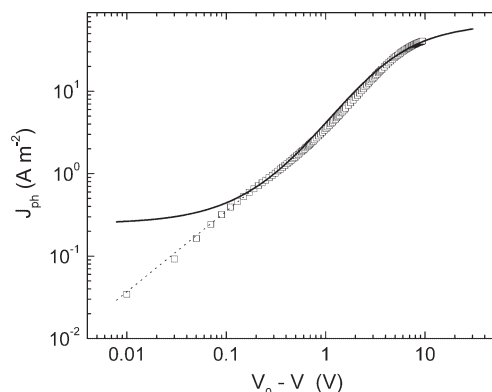


**Figure 2.** Photocurrent versus effective applied voltage (symbols) of a typical MDMO-PPV:PCNEPV solar cell, with an active layer thickness of 50 nm. The dotted line is a guide to the eye, showing the dependence on voltage with a slope of 1. The solid line is the calculated dissociation efficiency in this case.

zero.<sup>[9]</sup> In MDMO-PPV:PCBM (1:4 weight ratio) solar cells, the photocurrent linearly increases with voltage at a voltage close to the compensation voltage  $V_0$  ( $V_0 - V < 0.1 \text{ V}$ ) due to a competition between drift and diffusion currents. For  $V_0 - V > 0.1 \text{ V}$ , the photocurrent enters the saturation regime where it can be approximated by  $J_{ph} = eG(E,T)L$ , where  $e$  is the elementary charge,  $G(E,T)$  is the generation rate of free carriers ( $E$  and  $T$  are the electric field and temperature, respectively), and  $L$  is the sample thickness.<sup>[9]</sup> The rate  $G(E,T)$  is governed by the dissociation efficiency of the bound e-h pairs, which is a field- and temperature-dependent process.

As shown in Figure 2, these two regimes also occur in the MDMO-PPV:PCNEPV solar cells: a linear regime for  $V_0 - V < 0.1 \text{ V}$  (dotted line), where carrier drift and diffusion compete, followed by an S-shape-like regime (solid line) for  $V_0 - V > 0.1 \text{ V}$ . Such an S-shape of the photocurrent versus effective voltage is characteristic of the field-dependent dissociation process of bound e-h pairs; at low (or zero) field there is still dissociation of bound pairs taking place via thermal excitation (as is also evident from Equation 3 when  $b \rightarrow 0$ ; see later). However, compared to the MDMO-PPV:PCBM cells, the dissociation efficiency at low effective voltages in the all-polymer MDMO-PPV:PCNEPV cells is much lower. In MDMO-PPV:PCBM the difference between the dissociation at low fields ( $V_0 - V \approx 0.1 \text{ V}$ ) and at full saturation at high fields ( $V_0 - V \approx 0 \text{ V}$ ) is typically a factor of three, meaning that a third of the bound e-h pairs are already dissociated at low fields. From Figure 2 it appears that

the difference in the all-polymer cell is much larger, and typically amounts to two orders of magnitude. So only a small fraction of the created e–h pairs actually contributes to the photocurrent at low voltages. It is evident that such a low dissociation efficiency is responsible for a strongly reduced photocurrent. Furthermore, the strong field dependence and resulting inward bend in the fourth quadrant (Fig. 2) strongly suppresses the FF. The major question now is why the dissociation is so poor in these all-polymer solar cells.

## 2.2 Dissociation Efficiency

Because of the strong Coulomb binding energy in organic solar cells, only a certain fraction of the photogenerated bound e–h pairs  $G_{\max}$  are dissociated into free charge carriers, depending on the field and temperature, and therefore contribute to the photocurrent ( $eGL$ ). Consequently, the generation rate  $G$  of free charge carriers can be described by

$$G(T, E) = G_{\max} P(T, E) \quad 1$$

where  $P(T, E)$  is the probability for charge separation at the donor/acceptor interface. As stated above, the photogeneration of free charge carriers in low-mobility materials can be explained by the geminate recombination theory of Onsager.<sup>[12]</sup> An important addition to the theory was made by Braun,<sup>[13]</sup> who stressed the importance of the fact that the bound e–h pair (or charge transfer state) has a finite lifetime. In Braun's model, the probability that a bound polaron pair dissociates into free charge carriers at a given electric field  $E$  and temperature  $T$  is given by

$$P(T, E) = \frac{k_D(E)}{k_D(E) + k_F} \quad 2$$

where  $k_F$  is the rate constant for the bound e–h pair decaying to the ground state, and  $k_D(E)$  is the rate constant for their separation into free carriers, which is given by<sup>[13]</sup>

$$k_D = k_R \frac{3}{4\pi a^3} e^{-E_b/kT} \left[ 1 + b + \frac{b^2}{3} + \frac{b^3}{18} + \frac{b^4}{180} + \dots \right] \quad 3$$

where  $a$  is the initial separation distance of the bound e–h pair at the interface,  $b = e^3 E / 8\pi \epsilon_0 \epsilon_r k^2 T^2$  ( $\epsilon_0$  is the permittivity of free space), and  $E_b$  is the binding energy of the e–h pair.

Once separated, the charge carriers can again form a bound pair with a rate constant  $k_R$ . Using the Onsager theory for the field-dependent dissociation rate constants of weak electrolytes<sup>[12]</sup> for  $k_D(E)$ , Langevin recombination of free electrons and holes, and a Gaussian distribution of donor–acceptor distances, the generation rate of producing free electrons and holes depends on the charge-carrier mobilities,  $\mu_n$  and  $\mu_p$ , of the electron and holes, respectively, the relative dielectric constant  $\epsilon_r$ , the initial separation of e–h pairs  $a$ , and the ground-state recombination rate  $k_F$ . As a next step, we investigated the relevance of these parameters for dissociation in the MDMO-PPV:PCNEPV all-polymer cells.

In Figure 3 the dissociation probability  $P(E, T)$  is shown for a MDMO-PPV:PCBM (1:4 weight ratio) based solar cell (solid line). For this system, an initial e–h pair separation distance  $a = 1.3$  nm, a decay rate  $k_F = 1.0 \times 10^5$  s<sup>−1</sup>, a dielectric

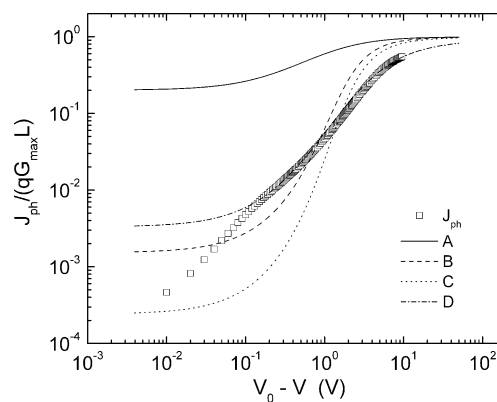


**Figure 3.** A) Calculated dissociation efficiency  $P(E, T)$  for a MDMO-PPV:PCBM solar cell (solid line), with a maximum generation rate  $G_{\max} = 2.7 \times 10^{27}$  m<sup>−3</sup> s<sup>−1</sup>, an initial e–h pair separation distance  $a = 1.3$  nm, a decay rate  $k_F = 1.0 \times 10^5$  s<sup>−1</sup>, a relative dielectric constant  $\epsilon_r = 3.4$ , and constant electron and hole mobilities  $\mu_n = 2.0 \times 10^{-7}$  m<sup>2</sup> V<sup>−1</sup> s<sup>−1</sup> and  $\mu_p = 2.0 \times 10^{-8}$  m<sup>2</sup> V<sup>−1</sup> s<sup>−1</sup>, respectively. B) The dashed line is the calculation with all the same generation parameters except for the carrier mobilities, which are equal to the ones of the MDMO-PCNEPV system,  $\mu_n = 6.0 \times 10^{-11}$  m<sup>2</sup> V<sup>−1</sup> s<sup>−1</sup> and  $\mu_p = 5.0 \times 10^{-10}$  m<sup>2</sup> V<sup>−1</sup> s<sup>−1</sup>. C) The dotted line is the calculation for the latter case with a spatial average dielectric constant for the polymeric system,  $\langle \epsilon_r \rangle = 2.6$ , also included. D) The dashed-dotted line shows  $P(E, T)$  for the all-polymer system using  $k_F = 1.0 \times 10^2$  s<sup>−1</sup> and  $a = 0.6$  nm. The active layer was assumed for all cases to be 50 nm. The symbols show the experimental MDMO-PPV:PCNEPV solar cell photocurrent, for an active layer of 50 nm.

constant  $\epsilon_r = 3.4$ , and electron and hole mobilities of  $\mu_n = 2.0 \times 10^{-7}$  m<sup>2</sup> V<sup>−1</sup> s<sup>−1</sup> and  $\mu_p = 2.0 \times 10^{-8}$  m<sup>2</sup> V<sup>−1</sup> s<sup>−1</sup> were used to describe the experiments.<sup>[14]</sup> In a recent study on the charge-transport properties of MDMO-PPV:PCNEPV (1:1 weight ratio) mobilities of  $\mu_n = 6.0 \times 10^{-11}$  m<sup>2</sup> V<sup>−1</sup> s<sup>−1</sup> and  $\mu_p = 5.0 \times 10^{-10}$  m<sup>2</sup> V<sup>−1</sup> s<sup>−1</sup> were measured.<sup>[11]</sup> As a first step we now included these lower mobility values in the calculation of  $P(E, T)$ , leaving all the other parameters equal to the MDMO-PPV:PCBM case (dashed line). At  $V_0 - V = 0.1$  V, the dissociation probability decreased from  $2.6 \times 10^{-1}$  to  $2.8 \times 10^{-3}$  because of the reduced mobilities in the all-polymer system. A beneficial effect of the dissociation in the MDMO-PPV:PCBM cells was that with increasing PCBM content the spatial average dielectric constant  $\langle \epsilon_r \rangle$  of the blend increased, because the  $\epsilon_r$  of 4.0 of PCBM is significantly larger than the 2.1 of MDMO-PPV.<sup>[14]</sup> At a 1:4 weight ratio this resulted in an average  $\langle \epsilon_r \rangle$  of 3.4. For the pristine PCNEPV we determined an  $\langle \epsilon_r \rangle$  of 3.2 from impedance measurements. In a 1:1 weight ratio of PCNEPV and MDMO-PPV in the blend, this resulted in an average  $\langle \epsilon_r \rangle$  of 2.6. The dotted line in Figure 3 shows the calculated dissociation probability  $P(E, T)$  with the reduced mobilities and also the reduced  $\langle \epsilon_r \rangle$  included. As a result, at  $V_0 - V = 0.1$  V  $P(E, T)$  further decreased to  $5.28 \times 10^{-4}$ , which lowered the photocurrent to values even below the experimentally observed ones.

As a final step we also modified the dissociation parameters  $a$  and  $k_f$  (dashed-dotted line): using  $k_f = 1 \times 10^2 \text{ s}^{-1}$  and  $a = 0.6 \text{ nm}$ , a good agreement with the experiment was obtained. Compared to the MDMO-PPV:PCBM blend, the separation distance between the bound e-h pair was strongly reduced, together with a decrease of its decay rate. This indicated that in the all-polymer blend the e-h pairs were strongly bound with a small separation distance, and a small decay rate, giving a long-lived charge-transfer state. It is evident that a small separation distance will lead to a reduced dissociation efficiency, because the Coulomb binding energy will strongly increase. For polymeric heterojunctions based on polyfluorenes, it is known that exciplexes are formed, indicative of a strong coupling between the electron and hole.<sup>[15]</sup> On the other hand, a strong coupling between the bound electron and hole is also expected to increase their recombination rate  $k_f$ . This increased recombination is in contrast to the small recombination rate that we obtain. An explanation might be that excitons are regenerated at these heterojunctions and, because of their long lifetime, can be back transferred into the bulk as an exciton.<sup>[15]</sup> Subsequently, part of these regenerated bulk excitons are dissociated again at the heterojunction, and again appear as bound pairs. In our dissociation model such an effect would show up as an increase of the effective lifetime of the bound pair.

In photophysical studies of the MDMO-PPV:PCNEPV blend, exciplex formation was also found by Offermans et al.; this formation was in competition with the formation of free-charge carriers, which can be described by the dissociation efficiency defined by Equation 2.<sup>[16]</sup> Probably, the small separation distance between the bound e-h pair in these all-polymer blends originates from the morphology of the films. In MDMO-PPV:PCBM (1:4 weight ratio) films, PCBM is known to form crystallites,<sup>[17]</sup> which might enhance the delocalization of the electrons. This would translate to a larger initial separation distance between the electrons and holes. In the MDMO-PPV:PCNEPV blend the phase separation is not as pronounced and the morphology is closer to a full intermixing on the molecular scale,<sup>[5]</sup> leading to smaller separation distances between the bound e-h pair.

### 2.3 The Photocurrent-Numerical Results

In order to model the photocurrent of the MDMO-PCNEPV solar cells we used a device model<sup>[18]</sup> that included drift and diffusion, the field- and temperature-dependent generation rate  $G(E, T)$ , and the carrier mobilities and trapping parameters as obtained from recent measurements.<sup>[11]</sup> In Figure 4 the measured and simulated photocurrents are shown. Because the simulations take into account that the electric field and the generation rate are not completely homogeneous, the dissociation parameters  $a$  and  $k_f$  have to be slightly adapted compared to Figure 3 to get the best fit.

The good agreement shows that the photocurrent of these all-polymer cells can be described within the same framework as the MDMO-PPV:PCBM cells. The major difference is the much smaller dissociation efficiency at low fields, also resulting in a steeper field dependence at higher voltage. It should also

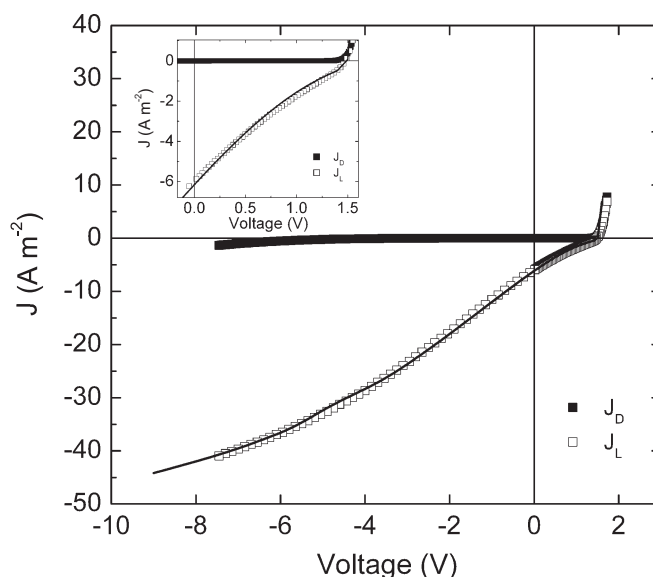


**Figure 4.** Dark (solid symbols) and illuminated (open symbols) characteristics of a MDMO-PPV:PCNEPV solar cell, with an active layer of 50 nm. The solid line is the calculated current with a maximum generation rate  $G_{\text{max}} = 9.3 \times 10^{27} \text{ m}^{-3} \text{ s}^{-1}$ , an e-h pair distance  $a = 0.62 \text{ nm}$ , a decay rate  $k_f = 7.0 \times 10^2 \text{ s}^{-1}$ , and carrier mobilities derived from transport measurements, with  $\mu_p = 5.0 \times 10^{-10} \text{ m}^2 \text{ V}^{-1} \text{ s}^{-1}$ , and  $\mu_n = 6.0 \times 10^{-11} \text{ m}^2 \text{ V}^{-1} \text{ s}^{-1}$ , and the electron-trapping parameters  $N_t = 9.6 \times 10^{22}$  and  $T_t = 2500 \text{ K}$ . The inset shows the magnified fourth quadrant of the  $J$ - $V$  plot.

be noted that the total amount of photogenerated e-h pairs  $G_{\text{max}} = 9.3 \times 10^{27} \text{ m}^{-3} \text{ s}^{-1}$ , as obtained from the saturated photocurrent at high reverse bias, is considerably larger than the MDMO-PPV:PCBM-based counterparts, where  $G_{\text{max}} = 2.5 \times 10^{27} \text{ m}^{-3} \text{ s}^{-1}$  was found.<sup>[14]</sup> Clearly, the all-polymer cells absorb more light, but the problem is to get the photogenerated electrons and holes separated. From the voltage dependence of the photocurrent, no space-charge effects seem to be present, their signature being a much lower dependence on voltage, with a slope of 0.5. This voltage dependence stems from the fact that in the case of carrier accumulation  $J_{\text{ph}} = eG(E, T)d$ , where  $d$  is the width accumulation region that is voltage dependent. To further verify that for  $V_0 - V > 1 \text{ V}$  the photocurrent is saturated and can be approximated by  $J_{\text{ph}} = eG(E, T)L$ , we also investigated the intensity dependence of the short-circuit current  $J_{\text{sc}}$ . In Figure 5, the measured short-circuit current is plotted as function of light intensity. The linear behavior obtained, as expected from  $eG(E, T)L$ , also shows that space-charge effects, which would give a slope of 0.75, do not play a role at short circuit in these devices.

As a last step, we also investigated the intensity dependence of the open-circuit voltage  $V_{\text{oc}}$ . It has been shown by Koster et al. that in the case of Langevin recombination, the open-circuit voltage  $V_{\text{oc}}$  of a solar cell depends linearly on the light intensity, with a slope of  $kT/q$ .<sup>[19]</sup> This was experimentally verified on various PPV-based fullerene systems. However, for the MDMO-PPV:PCNEPV solar cells, as shown in Figure 6, the experimental data showed a much steeper slope, whereas the calculated open-circuit voltage from the numerical device model with the parameters mentioned above had the expected  $kT/q$  slope.



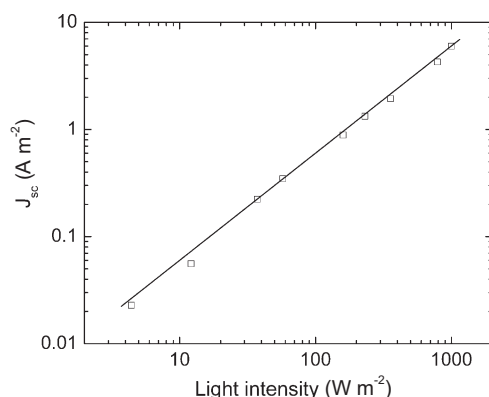


**Figure 5.** The dependence of the short-circuit current  $J_{sc}$  on the light intensity of a typical MDMO-PPV:PCNEPV solar cell (symbols) for an active layer of 50 nm. The solid line has a slope of 1, showing the linear dependence of  $J_{sc}$  on the light intensity.

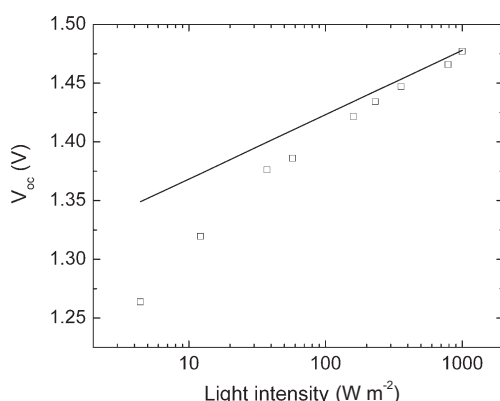


**Figure 6.** Experimental open-circuit voltage ( $V_{oc}$ ) of a typical MDMO-PPV:PCNEPV cell (symbols), with an active layer of 50 nm, and the calculation (line) with the parameters used to calculate the  $J$ - $V$  characteristic in case of Langevin recombination.

Apparently, in our model of the all-polymer cells there is still a process missing. At open circuit there is no current extraction and all the photogenerated charge carriers recombine.<sup>[18]</sup> As a result, the properties of the solar cell at open circuit are strongly dependent on the recombination processes. In a previous paper we demonstrated that electron transport in the PCNEPV phase is strongly trap-assisted.<sup>[11]</sup> In such a case, electrons are immobilized in the traps, and can, subsequently, recombine with free holes. Such a trap-assisted recombination path has not been included in the device model so far, because in the earlier studies on PPV-fullerene cells electron and hole transport could be regarded as trap-free. Trap-assisted recombination is described by the Shockley–Read–Hall (SRH) equation,<sup>[20,21]</sup> for which the recombination rate is given by<sup>[22]</sup>

$$R = C_n C_p N_t (pn - p_1 n_1) / [C_n (n + n_1) + C_p (p + p_1)] \quad 4$$

where  $C_n$  and  $C_p$  are the capture coefficients of electrons and of holes, respectively,  $N_t$  is the density of electron traps,  $n$  and  $p$  are the electron density in the conduction band and the hole

density in valence band, respectively, and  $p_1 n_1 = N_c N_v \exp[-(E_c - E_v)/kT] = n_i^2$  and is the intrinsic carrier concentration in the sample. In Figure 7 we show the influence of  $C_n$  and  $C_p$ , which are assumed to be equal (every trapped electron can capture a free hole), on the light-intensity dependence of the  $V_{oc}$ . Using  $C_n = C_p = 1.4 \times 10^{-18} \text{ m}^3 \text{ s}^{-1}$ , the light-intensity dependence of the  $V_{oc}$  is in agreement with the experiments. In this case, both Langevin and SRH recombination play a role in the solar cell.

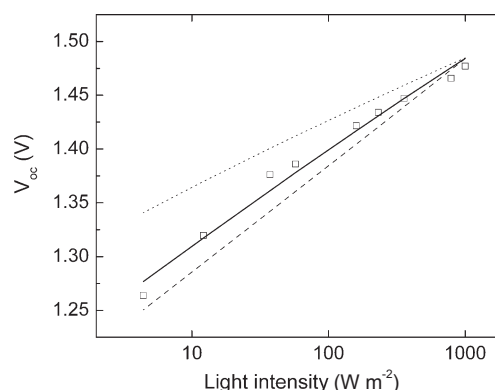


**Figure 7.**  $V_{oc}$  versus light intensity (symbols) of a typical MDMO-PPV:PCNEPV solar cell, with an active layer of 50 nm; and calculation (lines) using mobility values derived from transport measurements and the capture coefficients for electrons and holes  $C_n = C_p = 1.4 \times 10^{-18} \text{ m}^3 \text{ s}^{-1}$  (solid line),  $C_n = C_p = 5.0 \times 10^{-20} \text{ m}^3 \text{ s}^{-1}$  (dotted line) and  $C_n = C_p = 5.0 \times 10^{-17} \text{ m}^3 \text{ s}^{-1}$  (dashed line).

Including the trap-assisted recombination in the device model, we recalculated the photocurrent of the MDMO-PPV:PCNEPV all-polymer cell as shown in Figure 8. The dissociation parameters are not affected by the inclusion of the SRH recombination. As stated above, recombination is especially important at open circuit. However, at short circuit and in reverse bias almost all of the electrons and holes are extracted and recombination losses become negligible.

To understand the device operation it is important to know which recombination mechanism is responsible for the losses in the solar cell. As shown in Figure 9 the strength of the Langevin recombination is clearly dominant compared to the trap-limited SRH recombination at  $1000 \text{ W m}^{-2}$ . This is another reason why the inclusion of SRH recombination does not strongly affect the calculated photocurrent shown in Figure 4, where only Langevin recombination was taken into account. At lower light intensities ( $<100 \text{ W m}^{-2}$ ), trap-assisted recombination takes over from Langevin recombination because it has a weaker dependence on carrier density.

Thus, trapping effects are important at open-circuit voltage, but have only limited influence on the  $J$ - $V$  characteristics at normal and high light intensities. The assumption of a strongly bound e–h pair is necessary in both cases (trap-assisted recombination or not) in order to model the current under illumination.

We checked the validity of our model on a much thicker device, of 230 nm, as can be seen in Figure 10. The photocurrent

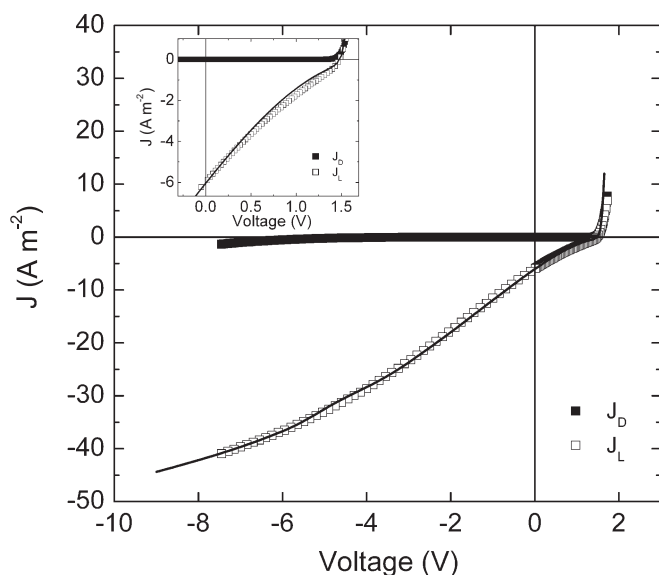


**Figure 8.** Dark (solid symbols) and illuminated (open symbols)  $J$ - $V$  characteristics of a MDMO-PPV:PCNEPV solar cell with an active layer of 50 nm. The solid line is the calculated current with a maximum generation rate  $G_{\max} = 9.4 \times 10^{27} \text{ m}^{-3} \text{ s}^{-1}$ , an e-h pair distance  $a = 0.62 \text{ nm}$ , a decay rate  $k_f = 6.7 \times 10^2 \text{ s}^{-1}$  and carrier mobilities derived from transport measurements, with  $\mu_p = 5.0 \times 10^{-10} \text{ m}^2 \text{ V}^{-1} \text{ s}^{-1}$ ,  $\mu_n = 6.0 \times 10^{-11} \text{ m}^2 \text{ V}^{-1} \text{ s}^{-1}$ , the electron-trapping parameters  $N_t = 9.6 \times 10^{22}$  and  $T_t = 2500 \text{ K}$ , and the capture coefficients  $C_n = C_p = 1.4 \times 10^{-18} \text{ m}^3 \text{ s}^{-1}$ . The inset shows the magnified fourth quadrant of the  $J$ - $V$  plot.

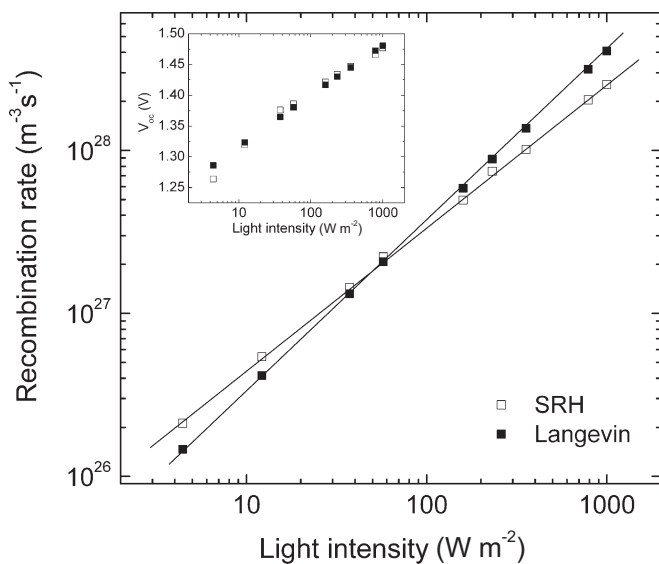


**Figure 9.** Rate of trap-assisted recombination (open symbols) and of Langevin recombination (solid symbols) as a function of light intensity, for the parameters used to calculate the current under illumination at  $1000 \text{ W m}^{-2}$ , with a field-dependent generation rate  $G$ . The solid lines are a guide to the eye. The inset shows the light-intensity dependence of the measured  $V_{oc}$  (open symbols) and the calculated values (solid symbols), corresponding to the calculated recombination rates.

can be modeled with all the parameters kept the same. The only correction made is for the maximum generation rate  $G_{\max}$ , which for thicker samples has a lower rate because it rep-

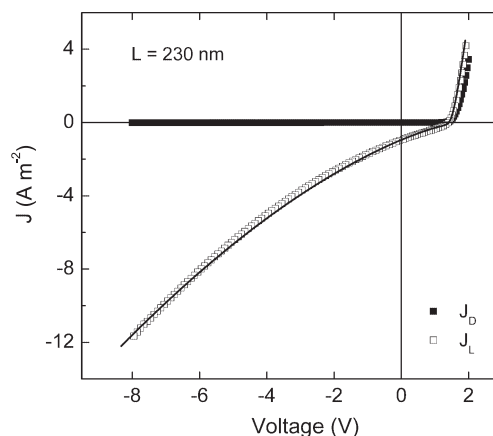


**Figure 10.** Dark (solid symbols) and illuminated (open symbols)  $J$ - $V$  characteristics of a MDMO-PPV:PCNEPV solar cell, with an active layer of 230 nm. The solid line is the calculated current with a maximum generation rate  $G_{\max} = 3.5 \times 10^{27} \text{ m}^{-3} \text{ s}^{-1}$ , an e-h pair distance  $a = 0.62 \text{ nm}$ , a decay rate  $k_f = 6.7 \times 10^2 \text{ s}^{-1}$ , and carrier mobilities derived from transport measurements with  $\mu_p = 5.0 \times 10^{-10} \text{ m}^2 \text{ V}^{-1} \text{ s}^{-1}$ ,  $\mu_n = 6.0 \times 10^{-11} \text{ m}^2 \text{ V}^{-1} \text{ s}^{-1}$ , electron-trapping parameters  $N_t = 9.6 \times 10^{22}$  and  $T_t = 2500 \text{ K}$ , and capture coefficients  $C_n = C_p = 1.4 \times 10^{-18} \text{ m}^3 \text{ s}^{-1}$ .

resents an average value over the sample thickness. In this case the rate amounts to  $3.5 \times 10^{27} \text{ m}^{-3} \text{ s}^{-1}$ . Trap-assisted recombination was included as well, with the same value for the capture coefficients as for the thin device of 50 nm.

The efficiency of this type of solar cell can be further increased by thermal treatment: annealing at  $120^\circ \text{C}$  for 15 min leads to an efficiency increase from 0.25 % to 0.5 %. Adding another acceptor layer increases the efficiency even further towards 0.75 %, as has been shown in Veenstra et al. For the unannealed devices, we have shown that the low FF and performance originates from a low dissociation efficiency. This poor dissociation is a combined effect of low mobility, low dielectric constant, and the small separation distance between electrons and holes (related to the morphology). As can be seen from Figure 11, annealing strongly changes the shape of the photocurrent. At high bias the photocurrents coincide, showing that

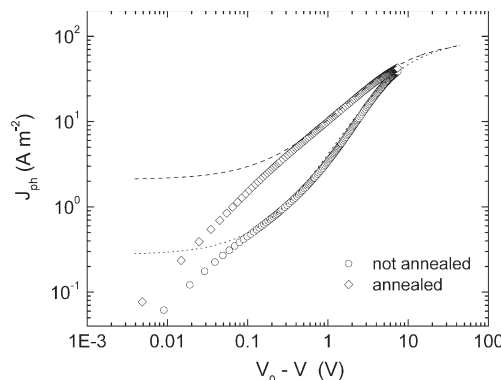


**Figure 11.** Photocurrent versus applied voltage for MDMO-PPV:PCNEPV solar cells, without thermal treatment (circles) and annealed at  $120^\circ \text{C}$  for 15 min (diamonds). The thickness of the active layer is in both cases around 40 nm. The dash and dotted line are a guide to the eye.

the amount of photogenerated e–h pairs have not changed. The change of the S-shape-like form indicates that annealing improves the dissociation efficiency in this type of cell. However, the main mechanism through which this improvement is achieved is not obvious: an increase in mobility, due to a better transport after annealing, a change in the dielectric constant, or a change in morphology upon annealing, facilitating the dissociation. This subject is presently under investigation.

### 3. Conclusion

We have investigated the photogeneration and recombination of charges in blends of all-polymer BHJ solar cells based on MDMO-PPV:PCNEPV. The electron traps present in the PCNEPV phase contribute to the recombination losses of the system at low light intensities. The trap-assisted recombination dominates the superlinear light-intensity dependence of the open-circuit voltage observed for this type of solar cell. However, at a light intensity of 1 Sun, the Langevin recombination is the main loss mechanism, dominating over the trap-assisted recombination. The photogenerated current is dominated by the poor dissociation efficiency of the strongly bound, long-lived electron–hole pairs. The combination of low carrier mobilities, low dielectric constant, and morphology gives rise to strongly field-dependent photogeneration efficiency, which explains the low photocurrents at operating voltages in the fourth quadrant, as well as the strongly reduced fill factor.

### 4. Experimental

The electron donor MDMO-PPV was synthesized using the sulfinyl route [23] yielding a molecular weight of  $300 \text{ kg mol}^{-1}$  and a polydispersity index of 2.7.

As electron acceptor, PCNEPV was synthesized as described elsewhere [24], with a molecular weight of  $73.4 \text{ kg mol}^{-1}$  and a polydispersity index of 3.3. The molecular weights and polydispersity indexes were measured against poly(styrene) standards.

The solar cells were prepared on ITO-coated glass substrates, provided by Philips Research. All substrates were cleaned, dried, and treated with UV–ozone prior to PEDOT:PSS (Bayer AG) spin-coating. After spin-coating, the PEDOT:PSS layer was dried at  $140^\circ\text{C}$  for 10 min, and, subsequently, the polymer blend was spin-coated from chlorobenzene solution in a nitrogen atmosphere. Subsequently, 1 nm of LiF, followed by 100 nm of Al, was deposited as a top electrode by using thermal evaporation at a chamber pressure of ca.  $10^{-6}$  mbar ( $1 \text{ mbar} = 100 \text{ Pa}$ ). The annealing of the devices was performed in a  $\text{N}_2$  atmosphere on a hot plate at  $120^\circ\text{C}$  for 15 min, before the deposition of the top electrode. The devices were characterized by using a Keithley 2400 SourceMeter, the measurements being performed under a nitrogen atmosphere. To measure the illuminated characteristics ( $J_L$ ), the

solar cells were illuminated through the ITO electrode with a white-light tungsten–halogen lamp, for which the intensity was set using a calibrated Si diode.

Received: November 17, 2006

Revised: March 2, 2007

Published online: July 24, 2007

- [1] W. Ma, C. Yang, X. Gong, K. Lee, A. J. Heeger, *Adv. Funct. Mat.* **2005**, *15*, 1617.
- [2] G. Li, V. Shrotriya, J. Huang, Y. Yao, T. Moriarty, K. Emery, Y. Yang, *Nat. Mater.* **2005**, *4*, 864.
- [3] M. Reyes-Reyes, K. Kim, and D. L. Carroll, *Appl. Phys. Lett.* **2005**, *87*, 083 506.
- [4] J. J. M. Halls, C. A. Walsh, N. C. Greenham, E. A. Marseglia, R. H. Friend, S. C. Moratti, A. B. Holmes, *Nature* **1995**, *376*, 498.
- [5] S. C. Veenstra, W. J. H. Verhees, J. M. Kroon, M. M. Koetse, J. Sweelssen, J. J. A. M. Bastiaansen, H. F. M. Schoo, X. Yang, A. Alexeev, J. Loos, U. S. Schubert, M. M. Wienk, *Chem. Mater.* **2004**, *16*, 2503.
- [6] M. M. Koetse, J. Sweelssen, K. T. Hoekerd, H. F. M. Schoo, S. C. Veenstra, J. M. Kroon, X. Yang, J. Loos, *Appl. Phys. Lett.* **2006**, *88*, 083 504.
- [7] T. Kietzke, H.-H. Hörhold, D. Neher, *Chem. Mater.* **2005**, *17*, 6532.
- [8] S. E. Shaheen, C. J. Brabec, N. S. Sariciftci, F. Padinger, T. Fromherz, J. C. Hummelen, *Appl. Phys. Lett.* **2001**, *78*, 841.
- [9] V. D. Mihailetschi, L. J. A. Koster, J. C. Hummelen, P. W. M. Blom, *Phys. Rev. Lett.* **2004**, *93*, 216 601.
- [10] V. D. Mihailetschi, J. Wildeman, P. W. M. Blom, *Phys. Rev. Lett.* **2005**, *94*, 126 602.
- [11] M. M. Mandoc, W. Veurman, L. J. A. Koster, M. M. Koetse, J. Sweelssen, B. de Boer, P. W. M. Blom, *J. Appl. Phys.* **2007**, *101*, 104 512.
- [12] L. Onsager, *J. Chem. Phys.* **1934**, *2*, 599.
- [13] C. L. Braun, *J. Chem. Phys.* **1984**, *80*, 4157.
- [14] V. D. Mihailetschi, L. J. A. Koster, P. W. M. Blom, C. Melzer, B. de Boer, J. K. J. van Duren, R. A. J. Janssen, *Adv. Funct. Mat.* **2005**, *15*, 795.
- [15] A. C. Morteani, P. Sreearunothai, L. M. Herz, R. H. Friend, C. Silva, *Phys. Rev. Lett.* **2004**, *92*, 247 402.
- [16] T. Offermans, P. A. van Hall, S. C. J. Meskers, M. M. Koetse, R. A. J. Janssen, *Phys. Rev. B: Condens. Matter Mater. Phys.* **2005**, *72*, 045 213.
- [17] J. K. J. van Duren, X. Yang, J. Loos, C. W. T. Bulle-Lieuwma, A. B. Sieval, J. C. Hummelen, R. A. J. Janssen, *Adv. Funct. Mater.* **2004**, *14*, 425.
- [18] L. J. A. Koster, E. C. P. Smits, V. D. Mihailetschi, P. W. M. Blom, *Phys. Rev. B: Condens. Matter Mater. Phys.* **2005**, *72*, 085 205.
- [19] L. J. A. Koster, V. D. Mihailetschi, R. Ramaker, P. W. M. Blom, *Appl. Phys. Lett.* **2005**, *86*, 123 509.
- [20] W. Shockley, W. T. Read, *Phys. Rev.* **1952**, *87*, 835.
- [21] R. N. Hall, *Phys. Rev.* **1952**, *87*, 387.
- [22] K. C. Kao, W. Hwang, *Electrical Transport in Solids*, Pergamon Press, Oxford **1981**.
- [23] L. Lutsen, P. Adriaenssens, H. Becker, A. J. van Breemen, D. Vanderzande, J. Gelan, *Macromolecules* **1999**, *32*, 6517.
- [24] M. M. Koetse, J. Sweelssen, T. Franse, S. C. Veenstra, J. M. Kroon, X. Yang, A. Alexeev, J. Loos, U. S. Schubert, H. F. M. Schoo, *Proc. SPIE-Int. Soc. Opt. Eng.* **2004**, 5215.